atmosphere

MDPI

Article

Seasonal Variations and Correlation Analysis of Water-Soluble Inorganic Ions in $PM_{2.5}$ in Wuhan, 2013

Ting Huang [1,2], Juan Chen [1], Weituo Zhao [1], Jixiong Cheng [3] and Shenggao Cheng [1,*]

1 School of Environmental Studies, China University of Geosciences, Wuhan 430074, China; 13476812887@163.com (T.H.); qq906004119@163.com (J.C.); weituo2006@126.com (W.Z.)
2 Department of Environmental Studies, SIP-UCLA Institute for Technology Advancement, Suzhou 215000, China
3 Hubei Environment Monitoring Center, Wuhan 430072, China; cjx_0125@163.com
* Correspondence: chengsg@cug.edu.cn; Tel./Fax: +86-27-6788-5178

Academic Editor: Robert W. Talbot
Received: 23 December 2015 ; Accepted: 14 March 2016 ; Published: 23 March 2016

Abstract: Daily $PM_{2.5}$ and water-soluble inorganic ions (NH_4^+, SO_4^{2-}, NO_3^-, Cl^-, Ca^{2+}, Na^+, K^+, Mg^{2+}) were collected at the Hongshan Air Monitoring Station at the China University of Geosciences (Wuhan) (30°31′N, 114°23′E), Wuhan, from 1 January to 30 December 2013. A total of 52 effective $PM_{2.5}$ samples were collected using medium flow membrane filter samplers, and the anionic and cationic ions were determined by ion chromatography and ICP, respectively. The results showed that the average mass concentration of the eight ions was 40.96 μg/m^3, which accounted for 62% of the entire mass concentration. In addition, the order of the ion concentrations was SO_4^{2-} > NO_3^- > NH_4^+ > Cl^- >K^+ > Ca^{2+} > Na^+ > Mg^{2+}. The secondary inorganic species SO_4^{2-}, NO_3^- and NH_4^+ were the major components of water-soluble ions in $PM_{2.5}$, with a concentration of 92% of the total ions of $PM_{2.5}$, and the total concentrations of the three ions in the four seasons in descending order as follows: winter, spring, autumn, and summer. NH_4^+ had a significant correlation with SO_4^{2-} and NO_3^-, and the highest correlation coefficients were 0.943 and 0.923 (in winter), while the minimum coefficients were 0.683 and 0.610 (in summer). The main particles were $(NH_4)_2SO_4$ and NH_4NO_3 in $PM_{2.5}$. The charge of the water-soluble ions was nearly balanced in $PM_{2.5}$, and the pertinence coefficients of water-soluble anions and cations were more than 0.9. The highest pertinence coefficients were in the spring (0.9887), and the minimum was in summer (0.9459). That is, there were more complicated ions in $PM_{2.5}$ in the summer. The mean value of NO_3^-/SO_4^{2-} was 0.64, indicating that stationary sources of $PM_{2.5}$ had a greater contribution in Wuhan.

Keywords: $PM_{2.5}$; water-soluble ions; correlation analysis; charge balance; Wuhan

1. Introduction

With the rapid development of modern industrialization and urbanization and the sustainable growth of energy consumption and the number of motor vehicles, air contamination has gradually become the core constraint of sustainable urban progress and eco-civilization construction in recent decades. As a vital indicator of current domestic ambient air quality, Particulate Matter (PM) with aerodynamic diameters less than 2.5 μm ($PM_{2.5}$) has received extensive attention from society and academia. $PM_{2.5}$ not only reduces atmospheric visibility [1,2] but also severely damages organisms in the environment and public health [3,4]. Numerous studies have revealed that the sources, material compositions and formation mechanisms of atmospheric $PM_{2.5}$ are very complicated [5,6], and $PM_{2.5}$ mainly contains black carbon [7], elemental carbon [8], crust elements [9,10], water-soluble ions [11,12], microelements [13,14], *etc*. Among these species, water-soluble ions could account for more than 80% of $PM_{2.5}$'s constituents [15] and are an important factor in the increase in $PM_{2.5}$ concentrations.

Nonetheless, $PM_{2.5}$'s constituents are different with the diversities of regional geographic conditions, meteorological conditions [16] and energy structures [17], and the constituents in the same district even show different varieties because of different economic development levels during different periods. The differences in $PM_{2.5}$ are primarily observed on the sources, composition structure, and concentration levels.

Wuhan is one of the most rapidly developing cities in China. Along with the increase in the speed of the urbanization process, the population is rising sharply, traffic pressure is constantly increasing, and problems from $PM_{2.5}$ pollution are also increasing gradually. Wuhan, as well as substantial areas of China, is experiencing chronic air pollution [18]. Currently, there are some preliminary studies on the composition characteristics and concentration levels of water-soluble ions in $PM_{2.5}$ in Wuhan [19–22]. However, these studies lack long-term and continuous monitoring data and a comparison of seasonal differences. Based on this background, this study monitored $PM_{2.5}$'s water-soluble ions in Wuhan continuously throughout an entire year from 1 January to 30 December 2013, and then analyzed the concentration levels and correlations of water-soluble ions and the seasonal variation in the main ions in order to provide a theoretical foundation for the control and treatment of $PM_{2.5}$ pollution in Wuhan.

2. Materials and Methods

2.1. Overview of the Study Area

Wuhan is located in the middle and lower reaches of the Yangtze River, east of the Jianghan Plain, and its geographical location is between 113°41′E and 115°05′E (longitude) and between 29°58′N and 31°22′N (latitude). The climate is a subtropical humid monsoon climate, with abundant rainfall, sufficient sunshine, and four distinct seasons; in the summer, the temperature is high and precipitation is concentrated, while in the winter, the weather is moist and slightly cold. The average temperature reaches the lowest point of 3.0 °C in January and a peak of 29.3 °C in July. The summer period is as long as 135 days, and the spring and autumn periods both contain approximately 60 days. Wet and dry seasons are readily apparent, the rainfall is relatively adequate in the early summer, and the annual precipitation is 1205 mm. According to the ground monitoring datum in Wuhan, the winter has a prevailing north-northeast wind (NNE), while the summer has a prevailing south-southwest wind (SSW), and the rest of the seasons have a dominant southwest wind. The annual average wind speed is 1.1–1.2 m/s, and light wind and calm wind are frequent. Air pollutants in northeastern provinces and cities easily drift to Wuhan with the airflow direction because of the controlled northeast monsoon in the winter, which could intensify Wuhan's air pollution. Therefore, Wuhan's air pollution is more serious in the winter than in other seasons. The wind rose diagram in Wuhan in 2013 is shown in Figure 1.

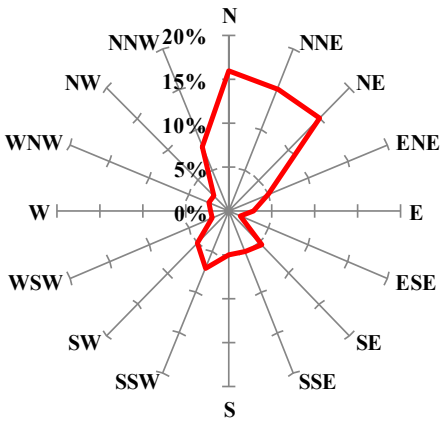

Figure 1. The wind rose diagram in 2013, Wuhan (calm wind frequency was 2.15%) 2.2 Sampling site and method.

The sampling site is on the roof of the Institute of Atmospheric Environment at the China University of Geosciences, Hongshan District of Wuhan (14°23′E, 30°31′N), at an elevation of approximately 8 m above the ground (Figure 2). From 1 January to 30 December 2014, we collected $PM_{2.5}$ samples continuously and acquired 52 valid samples with Wuhan Tianhong Company's sampling apparatus (Type TH-150F). The sampling filter used a quartz fiber filter membrane (QFF, Φ90 mm, Whatman Company, Leicestershire, UK). The sampling time started at 10 a.m. on each Wednesday and was maintained for 24 h to the next day.

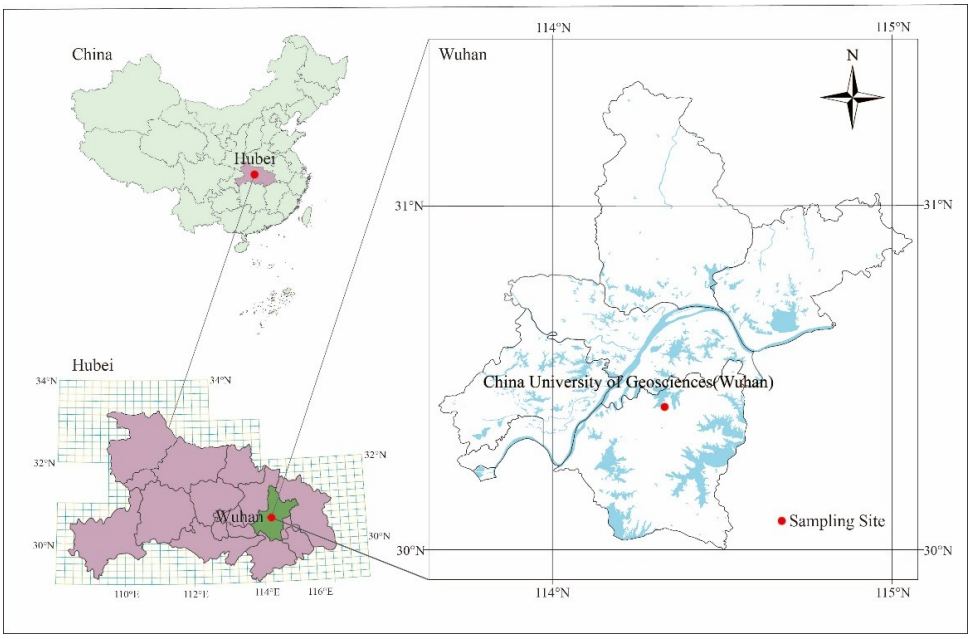

Figure 2. The location map of sampling site.

2.2. Sample Analysis Method

The $PM_{2.5}$ samples were weighed, and a quarter of the samples were cut up and placed into 50 mL polypropylene centrifugal tubes, to which was added 30 mL of ultrapure water. The samples were extracted at a constant temperature with an ultrasonic wave for 30 min and then stewed and filtered through a 0.45-μm-diameter micro-porous membrane. Furthermore, an inductively coupled plasma optical atomic emission spectrometer (Type ICAP6300, Thermo Fisher Scientific Inc, MA, USA) and an ion chromatograph (Type ICS-1100) were used to measure the concentrations of cations (K^+, Ca^{2+}, Na^+, Mg^{2+}, NH_4^+) and anions (Cl^-, SO_4^{2-}, NO_3^-). Stringent quality checks were executed during the sample analysis processes.

3. Results and Discussion

3.1. Concentration Level Analysis of $PM_{2.5}$'s Water-Soluble Ions

During the monitoring period, the total mass concentration value of the eight water-soluble ions of $PM_{2.5}$ was 40.96 μg/m^3, which accounted for 62% of the entire mass concentration. The sequence of the concentrations of water-soluble ions in order from high to low was $SO_4^{2-} > NO_3^- > NH^{4+} > Cl^- > K^+ > Ca^{2+} > Na^+ > Mg^{2+}$, and the three secondary ions SO_4^{2-}, NH_4^+ and NO_3^- were the main water-soluble ions, which were separately converted from gas precursors SO_2, NO_x and NH_3 and accounted for 92% of the total measured water-soluble ions.

The concentration level of SO_4^{2-} was the highest of the eight water-soluble ions and was lower than the values for the northern cities Beijing and Tianjin and greater than the values for the southern cities Shanghai, Guangzhou and Hong Kong (Table 1, [15,23–27]), mainly due to the emissions of

industrial pollution sources and coal sources in Wuhan. The concentration levels of NO_3^- and NH_4^+ ions were basically identical to the concentration of SO_4^{2-}. The high concentration of NO_3^- was based on the number of motor vehicles rising constantly in Wuhan in recent years. For example, take the NOx emissions (Table 2), we can find that the industrial NOx emission (stationary source) was the main source of NOx. Among them, NOx emission from thermal power industry was the primary source of pollution and accounts for 35.06% in the total NOx emission, followed by vehicle exhaust emissions accounts for 34%, suggesting that NOx emissions have a tendency to increase gradually. In addition, as seen from the seasonal distribution of NO_3^-, the concentration level in the winter and autumn was significantly higher than that in the spring and summer because the high temperatures in the spring and summer accelerated the volatilization loss of nitrate.

The annual average concentration of NH_4^+ in the study was second only to that of Beijing and was relatively high in the winter and low in the summer. NH_4^+, converted from NH_3, is an important ion that reacts with SO_4^{2-} and NO_3^- in the aerosol phase to form secondary particles. NH_3 mainly comes from agricultural production, industrial emissions, vehicle exhaust emissions and other sources. Attributed to the sharp rise of motor vehicles in Wuhan, a large number of nitrogen compounds are emitted into atmosphere by vehicle exhaust and produce ammonium nitrate through a chemical reaction with NH_3. Meanwhile, urban population growth (increasing the consumption of energy) and industrial economic expansion (such as thermal power industry, iron and steel industry and cement industry) are also important factors leading to an increase in ammonia emissions.

Table 1. Mass concentration of particulate matter ($PM_{2.5}$) and the water-soluble ions at different sites ($\mu g/m^{-3}$).

Site	Wuhan (This Study)	Wuhan [23]	Beijing [15]	Shanghai [24]	Tianjin [25]	Hongkong [26]	Guangzhou [27]
Location	urban	urban	urban & suburb	urban	urban	urban	urban
Time	2013	2012	2012–2013	2003–2005	2008	2003	2012–2013
Sampling sites	1	2	8	2	1	1	1
Sample number	52	21	519	202	19	–	51
$PM_{2.5}$	65	120.91	89.8	94.6	144.6	49.3	76.8
Cl^-	1.24	2.18	3.61	3	6.7	0.17	1.8
NO_3^-	11.28	25.61	20.3	6.32	16.6	0.79	7.8
SO_4^{2-}	16.78	43.15	19.4	10.39	24.1	11.6	18.1
NH_4^+	9.67	17.83	13.5	3.78	8.7	4.3	5.1
Na^+	0.24	0.75	1.19	0.57	3.4	0.26	2.2
K^+	1.08	2.96	1.05	0.63	0.9	0.67	0.9
Mg^{2+}	0.14	0.35	0.05	0.28	1	0.045	–
Ca^{2+}	0.54	5.17	0.78	1.25	1.8	0.13	–

Table 2. Main pollution source of NOx in Wuhan, 2013–2014 [28].

Year	2013		2014	
Sources	**Emissions (t)**	**Percentage (%)**	**Emissions (t)**	**Percentage (%)**
Total NOx emission	147,100	–	137,000	–
Total industrial NOx emission	95,600	65.00	84,200	61.46
Thermal power industry	51,576	35.06	29,817	21.80
Iron and steel industry	9937	6.76	9661	7.05
Cement industry	7340	5.00	6580	4.80
Vehicle exhaust emissions	50,000	34.00	51,400	37.54
Life source emissions	1400	0.95	1300	0.95
Centralized management facilities	100	0.05	100	0.05

3.2. Seasonal Variation Characteristics of Water-Soluble Ions

The mass concentration variation of water-soluble ions in $PM_{2.5}$ presented distinctly seasonal distribution features. The sequence of the mass concentration levels in the four seasons was

winter > spring > autumn > summer. The seasonal distribution of the cumulative concentration of eight water-soluble ions is shown in Figure 3. The concentration sum of the three main secondary ions (SO_4^{2-}, NO_3^-, NH_4^+) in the four seasons accounted for 79%, 46%, 67% and 85% of the total soluble-water ions, respectively, and was highest in the winter. The average mass concentration of the eight ions was 40.96 μg/m^3, which composed 63% of the total mass concentration of the water-soluble ions.

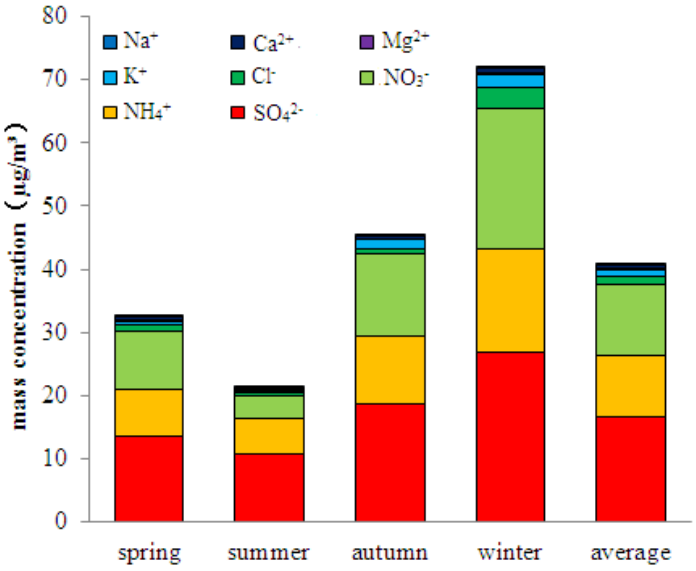

Figure 3. Seasonal variation of water-soluble ions in Wuhan during the observation period.

As shown in Figure 4, the proportion of concentration contribution of the three main ions was SO_4^{2-} (31.64%) > NO_3^- (26.27%) > NH_4^+ (19.27%) in winter, and the same order in spring and autumn, but was SO_4^{2-} (23.11%) > NH_4^+ (12.15%) > NO_3^- (7.38%) in summer, implying concentration value of NH_4^+ was ascending comparing with the value of NO_3^-. High temperature in summer is advantageous for the decomposition of solid material NH_4NO_3 and forming into gaseous materials NH_3 and HNO_3. After two-step chemical reactions (step one: $NH_3 + H_2O = NH_3 \cdot H_2O$; step two: $NH_3 \cdot H_2O = NH_4^+ + OH^-$) in the atmosphere, NH_3 transforms into NH_4^+ compounds, causing the concentration level of NH_4^+ to rise.

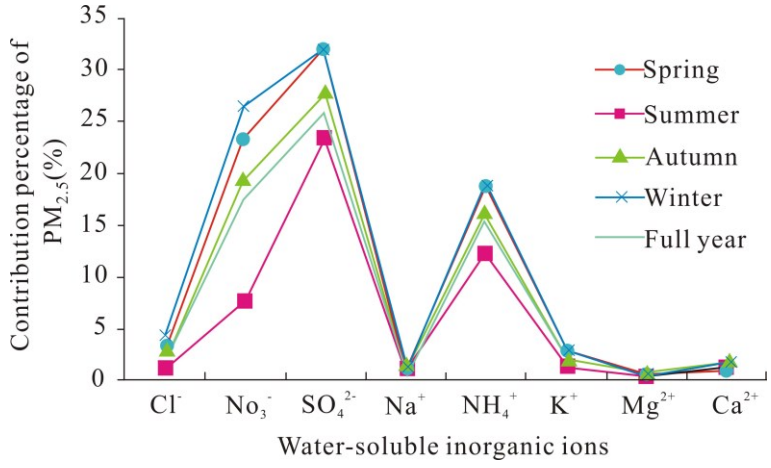

Figure 4. Seasonal variation of eight inorganic ions accounts for the total mass concentration of $PM_{2.5}$ in Wuhan during observation period.

Similar to the seasonal variation tendency of all water-soluble ions, the concentration of SO_4^{2-} was greatest in the winter, followed by the autumn, and was the lowest in the summer. The concentration value in the winter was 2.5 times that of the summer. One reason for the above situation is that citizens generally burn coal to keep warm in the winter. In addition, little rain and a dry climate in the winter cause SO_4^{2-} to remain in the atmosphere for a long time, so its concentration is elevated. On the contrary, high temperatures and rainy weather in the summer are not conducive to the formation of SO_4^{2-}.

The concentration levels of Ca^{2+} and Mg^{2+} experienced similar seasonal varying trends, such that the values decreased as follows: winter > autumn > spring > summer. The concentrations of Ca^{2+} and Mg^{2+} in the winter were 1.9 times and 4.3 times those of the summer, respectively. As typical ions of flowing dust [29], the concentrations of Ca^{2+} and Mg^{2+} are immensely influenced by seasons and anthropic actions. On one hand, the winter climate with dry weather and little rain reduces wet subsidence of Ca^{2+} and Mg^{2+}; on the other hand, with accelerating urbanization processes in recent years in Wuhan, a large number of surfaces from construction operation are emerging every year, thus increasing dust sources and resulting in the rise in the concentrations of Ca^{2+} and Mg^{2+} ions. Conversely, high temperatures and rainy weather in the summer provide beneficial conditions for the settlement of Ca^{2+} and Mg^{2+} compounds, which causes the concentrations of Ca^{2+} and Mg^{2+} ions to drop.

3.3. Concentration Equivalent Ratio Analysis of NO_3^-/SO_4^{2-}

Concentration equivalent normality is defined as the number of equivalents per liter of solution, where the definition of an equivalent depends on the reaction taking place in the solution. For an acid-base reaction, the equivalent is the mass of the acid or base that can furnish or accept exactly 1 mole of protons (H+ ions). The mass concentration equivalent ratio of NO_3^- and SO_4^{2-} could be used as relative significant index to measure the relative contribution of mobile source (vehicles) and fixed sources (coal) for nitrogen pollution and sulfur pollution in the atmosphere [24]. Arimoto *et al.* (1996) attributed the high ratio of NO_3^-/SO_4^{2-} to mobile sources, which had a greater contribution to the concentrations of regional atmospheric pollutants [30]. The sulfur contents in gasoline and diesel in China were 0.12% and 0.2%, respectively. The NO_x/SO_x ratios from comburent of gasoline and diesel fuel were approximately 13:1 and 8:1, respectively. Coal's sulfur content is 1%; the ratio of NO_X/SO_X from coal's combustion is approximately 1:2. Therefore, NO_X and SO_X can act as tracers of mobile sources and fixed sources separately. When the concentration equivalent ratio of NO_3^-/SO_4^{2-} exceeds 1, it means that pollution sources of the observation point are dominated by mobile sources, while fixed sources play major roles when the ratio is below 1 [30]. The equivalent ratios of NO_3^-/SO_4^{2-} in Wuhan were 0.73, 0.32, 0.70 and 0.83 in the spring, summer, autumn and winter, respectively. The annual average equivalent ratio of NO_3^-/SO_4^{2-} in Wuhan was 0.64, which is higher than the value of 0.73 in Changbai Mountain and the value of 0.46 in Nanjing, lower than the value of 0.83 in Shanghai, and essentially consistent with the value of 0.64 in Beijing [31]. The results revealed that the main pollution source in Wuhan was a fixed pollution source, which was consistent with the research of Zhang *et al.* [22].

3.4. Charge Balance Analysis of Water-Soluble Ions

Previous studies showed that the charge balance of water-soluble ions in $PM_{2.5}$ could be used to analyze the importance of the contribution of water-soluble ions to the mass concentration of $PM_{2.5}$ [14,32,33]. According to the analysis of data from the experiments, the charge balance figures of $PM_{2.5}$'s anions and cations in the four seasons in 2013 are drawn in Figure 5.

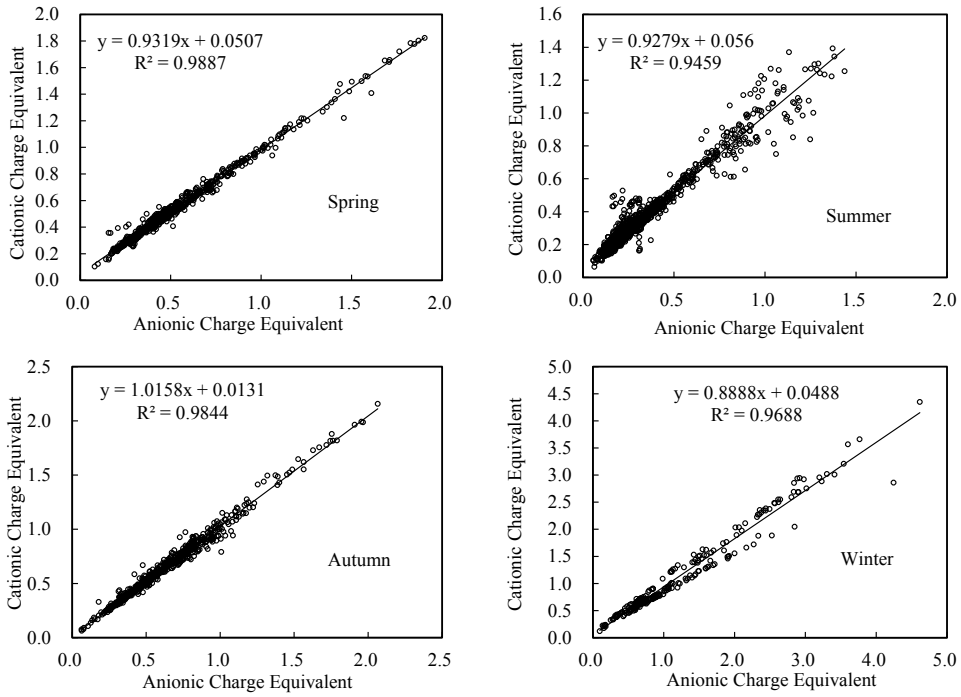

Figure 5. The charge balance of anion and cation water-soluble ions in Wuhan in four seasons.

The slope value of the linear fitting lines reached 0.9319 (R^2 = 0.9887), 0.9279 (R^2 = 0.9459) and 1.0158 (R^2 = 0.9844) in spring, summer and autumn, respectively. All values were nearly 1, while the slope value in winter only reached 0.8888 (R^2 = 0.9688), and had a relatively large gap with 1. These results revealed that the main ionic compositions in $PM_{2.5}$ in spring, summer and autumn were SO_4^{2-}, NO_3^-, Cl^-, Na^+, K^+, NH_4^+, Mg^{2+} and Ca^{2+}, the eight ions that the experiments analyzed. By contrast, cationic charge numbers were slightly low in winter, revealing that there were some other cationic ions not detected except those had been measured in this study (Na^+, K^+, NH_4^+, Mg^{2+} and Ca^{2+}), such as H^+ [34], organic cations or heavy metal ions (Zn^{2+}, Cu^{2+}, *etc.*), which reflected that the ion components of $PM_{2.5}$ in winter were much more complicated than that in spring, summer and autumn, and resulted from the more serious air pollution problems in winter compared with other seasons. Morever, existing research have shown that the mass concentrations of PM were higher in winter than other seasons, hence it carried a certain probability that $PM_{2.5}$ contained organic cations [7] or heavy metal ions (Zn^{2+}, Cu^{2+}, *etc.*) in winter [35]. This is not only a significant feature of the $PM_{2.5}$ in winter, but also one of the reasons that the days of heavy pollution weather in winter were more than the days in the other three seasons.

3.5. Correlation and Seasonal Difference Analysis of Water-Soluble Ions

The existing forms of water-soluble ions in $PM_{2.5}$ are diverse in different air pollution extents or different seasons, which have certain effects on atmospheric visibility, the PH of particulate matter, the viability of chemical reactions, *etc.* The correlation analysis method is usually used to study the existing forms of water-soluble ions [36]. As the correlation coefficient between water-soluble ions increases, the correlation between water-soluble ions increases.

The Pearson correlation coefficients of the water-soluble ions of $PM_{2.5}$ in all four seasons are shown in Tables 3–6 below. High correlations existed between NH_4^+ and SO_4^{2-}, NH_4^+ and NO_3^-, Mg^{2+} and SO_4^{2-}, Ca^{2+} and SO_4^{2-}, K^+ and Cl^-, Na^+ and Cl^-, which were consistent overall in one season. Nevertheless, seasonal differences lie in water-soluble ions. The correlation levels between NH_4^+ and SO_4^{2-}, NH_4^+ and NO_3^- were significantly higher than the level in the summer, slightly exceeding the value in the autumn, while distinctly lower than the degree in the winter. The correlations between

Mg^{2+} and SO_4^{2-} were higher in the spring, summer and autumn, but not in the winter, according to the sequence that the correlation coefficient spring > summer > autumn > winter. The correlation between Mg^{2+} and Cl^- was higher than the level between Mg^{2+} and SO_4^{2-}. The correlation of Ca^{2+} and SO_4^{2-} followed the order of spring > autumn > summer > winter, and the correlation between Ca^{2+} and NO_3^- was higher than that between Ca^{2+} and SO_4^{2-}. The correlation between K^+ and Cl^- followed the order autumn > winter > spring, and the correlation level of K^+ and SO_4^{2-} was obvious than the level of K^+ and Cl^-. NH_4^+, SO_4^{2-} and NO_3^- in the weak acid environment is reversible reaction, and reaction process is as follows:

$$2NH_4^+ + SO_4^{2-} \leftrightarrow (NH_4)_2SO_4 \quad (1)$$

$$H^+ + 3NH_4^+ + 2SO_4^{2-} \leftrightarrow (NH_4)_3H(SO_4)_2 \quad (2)$$

$$NH_4^+ + NO_3^- \leftrightarrow NH_4NO_3 \quad (3)$$

NH_4^+ as a kind of weak acid ion, is an incomplete reaction in aqueous solution, which existing in free form has not been involved in the charge balance in the solution. In the acidic environment, we can ignore the effects of free NH_4^+ on the balance, the results as shown in Figure 6. Figure 6 presents the positive and negative charge balances of NH_4^+, SO_4^{2-} and NO_3^- in all four seasons. As is shown in these figures, the slope values (k) of the fitting line between the charge equivalent of NH_4^+ and the charge equivalent of SO_4^{2-}+NO_3^- were all less, but very close to, 1; meanwhile, the goodness of fit values (R^2) approximated 1. As a consequence, NH_4^+ in $PM_{2.5}$ in Wuhan was neutralized by SO_4^{2-} and NO_3^- in all four seasons in 2013, which then existed with the forms of $(NH_4)_2SO_4$, $(NH_4)_3H(SO_4)_2$and NH_4NO_3 in $PM_{2.5}$.

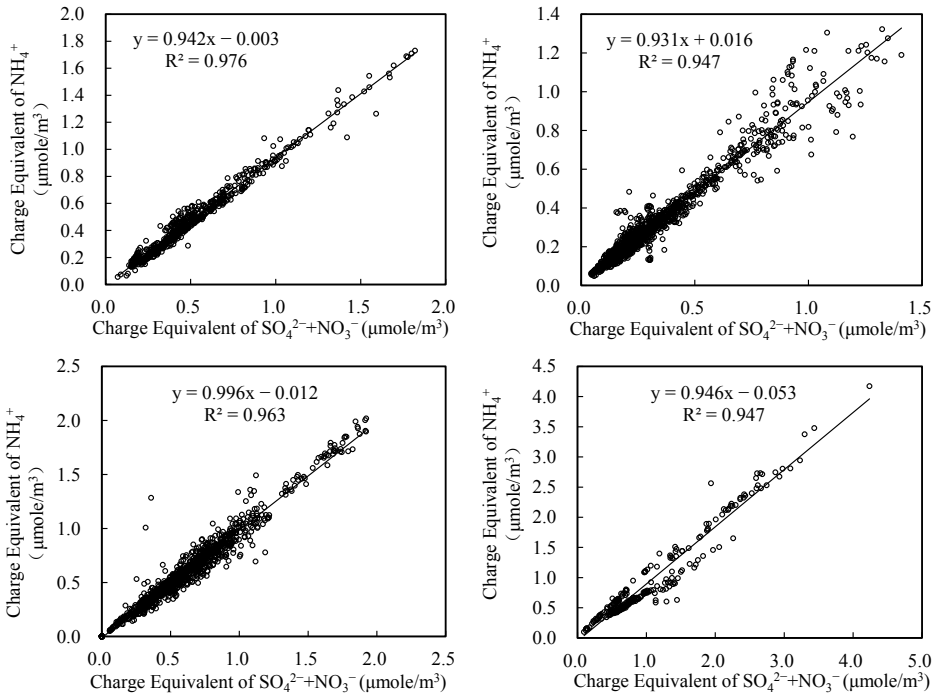

Figure 6. Positive and negative charge balances of NH_4^+, SO_4^{2-} and NO_3^- in all four seasons in Wuhan.

Synthetically, diverse forms of inorganic water-soluble ions in $PM_{2.5}$ not only have some similar states or common characteristics but also exists some variation in four different seasons in Wuhan. The similarity or consistency was revealed at the aspect that the main compositions of $PM_{2.5}$ were basically identical in four seasons, with their cations consisted of NH_4^+, Mg^{2+}, Ca^{2+}, K^+ and Na^+. In addition,

there were several kinds of same particles in the four seasons, including $(NH_4)_2SO_4$, NH_4NO_3 and $CaSO_4$. The variation or diversity was reflected by the types of main particles compositions of $PM_{2.5}$ in four seasons. Among them, Na^+ ion mainly composited to form NaCl in spring (correlation coefficient between Na^+ and Cl^- reached 0.458 in Table 3), while forming $NaNO_3$ in summer, autumn and winter (correlation coefficients between Na^+ and NO_3^- reached 0.423, 0.331 and 0.706 in Tables 4–6 respectively); K^+ composed to be K_2SO_4 in summer (correlation coefficient between K^+ and SO_4^{2-} reached 0.631 in Table 4), and then KCl in spring, autumn and winter (correlation coefficients between K^+ and Cl^- reached 0.537, 0.632 and 0.612 in Tables 3, 5 and 6, respectively); K^+ also formed KNO_3 only in autumn (correlation coefficient between K^+ and NO_3^- reached 0.586 in Table 5); Mg^{2+} composited $MgCl_2$ in winter (correlation coefficient between Mg^{2+} and Cl^- reached 0.331 in Table 6) while $MgSO_4$ in spring, summer and autumn (correlation coefficients between Mg^{2+} and SO_4^{2-} reached 0.590, 0.469 and 0.441 in Tables 3–5 respectively); furthermore, $Ca(NO_3)_2$ also came into being in winter as a compound of Ca^{2+}, with correlation coefficient between Ca^{2+} and NO_3^- reached 0.418 in Table 6, unlike other seasons that $CaSO_4$ was the main existing form.

Table 3. Pearson correlation of the water-soluble ions in $PM_{2.5}$ in the spring.

–	Cl^-	NO_3^-	SO_4^{2-}	Na^+	NH_4^+	K^+	Mg^{2+}	Ca^{2+}
Cl^-	1	–	–	–	–	–	–	–
NO_3^-	0.401 **	1	–	–	–	–	–	–
SO_4^{2-}	0.036	0.579 **	1	–	–	–	–	–
Na^+	**0.458** **	0.337 **	0.396 **	1	–	–	–	–
NH_4^+	0.276 **	**0.882** **	**0.859** **	0.371 **	1	–	–	–
K^+	**0.537** **	0.439 **	0.426 **	**0.811** **	0.492 **	1	–	–
Mg^{2+}	**0.152** **	0.082 *	**0.590** *	0.473 **	0.001	0.269 **	1	–
Ca^{2+}	0.085 *	−0.253 **	**0.536** **	0.382 **	−0.301 **	0.135 **	0.698 **	1

**: Significant at a level of 0.01 (2-tailed); *: Significant at a level of 0.05 (2-tailed); the bold data: descripted in content.

Table 4. Pearson correlation of the water-soluble ions in $PM_{2.5}$ in the summer.

–	Cl^-	NO_3^-	SO_4^{2-}	Na^+	NH_4^+	K^+	Mg^{2+}	Ca^{2+}
Cl^-	1	–	–	–	–	–	–	–
NO_3^-	0.668 **	1	–	–	–	–	–	–
SO_4^{2-}	0.293 **	0.335 **	1	–	–	–	–	–
Na^+	0.173 **	**0.423** **	0.159 **	1	–	–	–	–
NH_4^+	0.582 **	**0.611** **	**0.686** **	0.441 **	1	–	–	–
K^+	0.449 **	0.397 **	**0.631** **	0.211 **	0.659 **	1	–	–
Mg^{2+}	0.101 **	−0.089 **	**0.469** **	0.067 *	−0.116 **	0.092 **	1	–
Ca^{2+}	0.114 **	0.036	**0.438** **	0.291 **	0.134 **	0.311 **	0.125 **	1

**: Significant at a level of 0.01 (2-tailed); *: Significant at a level of 0.05 (2-tailed); the bold data: descripted in content.

Table 5. Pearson correlation of the water-soluble ions in $PM_{2.5}$ in the autumn.

–	Cl^-	NO_3^-	SO_4^{2-}	Na^+	NH_4^+	K^+	Mg^{2+}	Ca^{2+}
Cl^-	1	–	–	–	–	–	–	–
NO_3^-	0.552 **	1	–	–	–	–	–	–
SO_4^{2-}	0.177 **	0.472 **	1	–	–	–	–	–
Na^+	0.184 **	**0.331** **	0.224 **	1	–	–	–	–
NH_4^+	0.488 **	**0.846** **	**0.821** **	0.214 **	1	–	–	–
K^+	**0.632** **	**0.586** **	0.392 **	0.271 **	0.546 **	1	–	–
Mg^{2+}	0.111 **	0.235 **	**0.441** *	0.263 **	0.228 **	0.176 **	1	–
Ca^{2+}	−0.004	0.035	**0.502** **	0.682 **	0.001	0.184 **	0.218 **	1

**: Significant at a level of 0.01 (2-tailed); *: Significant at a level of 0.05 (2-tailed); the bold data: descripted in content.

Table 6. Pearson correlation of the water-soluble ions in $PM_{2.5}$ in the winter.

–	Cl^-	NO_3^-	SO_4^{2-}	Na^+	NH_4^+	K^+	Mg^{2+}	Ca^{2+}
Cl^-	1	–	–	–	–	–	–	–
NO_3^-	0.365 **	1	–	–	–	–	–	–
SO_4^{2-}	0.486 **	0.846 **	1	–	–	–	–	–
Na^+	0.306 **	**0.706 ** **	**0.695 ** **	1	–	–	–	–
NH_4^+	0.474 **	**0.925 ** **	**0.941 ** **	0.696 **	1	–	–	–
K^+	**0.612 ** **	0.436 **	0.518 **	0.528 **	0.395 **	1	–	–
Mg^{2+}	**0.331 ** **	0.021	0.141 *	0.214 **	−0.067	0.738 **	1	–
Ca^{2+}	−0.172 **	**0.418 ** **	**0.316 ** **	0.004	−0.421 **	−0.158 **	0.144 *	1

**: Significant at a level of 0.01 (2-tailed); *: Significant at a level of 0.05 (2-tailed); the bold data: descripted in content.

4. Conclusions

This study elucidated the characteristics of $PM_{2.5}$ in Wuhan city from January to December 2013. The analyses of the obtained results showed that there was a relatively high total mass concentration level of water-soluble ions in $PM_{2.5}$, and the ions followed a descending order of $SO_4^{2-} > NO_3^- > NH_4^+ > Cl^- > K^+ > Ca^{2+} > Na^+ > Mg^{2+}$. The dominant ions of SO_4^{2-}, NO_3^- and NH_4^+ had a total concentration that reached 92% of the total water-soluble ions of $PM_{2.5}$, which showed that secondary particle pollution in Wuhan was very serious. The mass concentration of water-soluble ions in $PM_{2.5}$ in four seasons followed the sequence of winter > spring > autumn > summer. The concentration of the main secondary ions SO_4^{2-}, NO_3^- and NH_4^+ relative to the concentration of the whole water-soluble ions in the spring, summer, autumn and winter were 79%, 46%, 67% and 85%, respectively, and the annual average concentration value of all water-soluble ions was 63%.

The charge balance fitting curves of water-soluble ions in $PM_{2.5}$ had a high degree of imitation, indicating that the positive and negative charges of water-soluble ions were essentially balanced. Among the ions, there were certain cationic losses in the summer. In addition, there were large differences in the types of water-soluble ions in $PM_{2.5}$ in the four seasons. The main molecular compositions of $PM_{2.5}$ were $(NH_4)_2SO_4$, NH_4NO_3, NaCl, $NaNO_3$, $NaSO_4$, KCl, K_2SO_4, KNO_3, $MgSO_4$, $MgCl_2$, $CaSO_4$ and $Ca(NO_3)_2$, and $(NH_4)_2SO_4$ and NH_4NO_3 were the dominant particles over the four seasons. The N and S emissions from human activities in Wuhan were large, and the main air pollution sources were inorganic secondary sources. In addition, the charge balance fitting curve in winter revealed that there were some other cationic ions not detected such as organic cations or heavy metal ions (Zn^{2+}, Cu^{2+}, *etc.*), which reflected that the ion components of $PM_{2.5}$ in winter was much more complicated than that in spring, summer and autumn. Therefore, for the further study, we must focus on the organic cations and heavy metal ions, especially in winter and the haze pollution weather. In addition, we also must realize that the temporal difference and seasonal difference in source apportionment of airborne particulate matter.

The mass concentration equivalent ratio of NO_3^-/SO_4^{2-} in the spring, summer, autumn and winter were 0.73, 0.32, 0.70 and 0.83, respectively, and the mean ratio was 0.64, which revealed that the main pollution sources (mobile source and stationary source) in Wuhan were fixed sources. The emissions load of fixed pollution sources in Wuhan, which is a vital industrial city, is relatively high from steel metallurgy, thermal power, cement and other industries. The city's industrial waste gas emissions reached 563.642 billion cubic meters 5636.42 (10^8 m^3) in 2013, and industrial SO_2 emissions and smoke powder accounted for 94.4% and 77.2% of the total emissions, respectively. With the background of energy conservation, emissions reduction and air quality improvement, relevant government departments and persons in Wuhan should strictly adopt the following measures: converting energy structures, improving industrial technologies, controlling the release of the fixed sources and normalizing the EIA approval process of air-involved construction projects. For motor vehicle exhaust pollution control, Wuhan have conducted the reform pilot work of Diesel Exhaust After treatment System Technical in 2015, adopting advanced technology to decrease the emission of

nitrogen oxides and particulate matter in addition to gradual elimination of Yellow Label cars and old cars by strict traffic law enforcement, in order to reduce the mobile sources of exhaust pollution.

Acknowledgments: This work was supported by the Natural Science Foundation of China (No. 41072023 and 41402312).

Author Contributions: Ting Huang and Shenggao Cheng designed the study, analyzed the data and wrote the manuscript. Juan Chen, Weituo Zhao and Jixiong Cheng collected the data, coordinated the data-analysis and revised the paper.

Conflicts of Interest: The authors declare no conflict of interest.

References

1. Yuan, C.S.; Lee, C.G.; Liu, S.H.; Chang, J.C.; Yuan, C.; Yang, H.Y. Correlation of atmospheric visibility with chemical composition of Kaohsiung aerosol. *Atmos. Environ.* **2006**, *82*, 663–679. [CrossRef]
2. Liao, W.H.; Wang, X.M.; Fan, Q.; Zhou, S.Z.; Chang, M.; Wang, Z.M.; Wang, Y.; Tu, Q.L. Long-term atmospheric visibility, sunshine duration and precipitation trends in South China. *Atmos. Environ.* **2015**, *107*, 204–216. [CrossRef]
3. Baker, K.R.; Foley, K.M. A nonlinear regression model estimating single source concentrations of primary and secondarily formed $PM_{2.5}$. *Atmos. Environ.* **2011**, *45*, 3758–3767. [CrossRef]
4. Yang, L.X.; Cheng, S.H.; Wang, X.F.; Nie, W.; Xu, P.J.; Gao, X.M.; Yuan, C.; Wang, W.X. Source identification and health impact of $PM_{2.5}$ in a heavily polluted urban atmosphere in China. *Atmos. Environ.* **2013**, *75*, 265–269. [CrossRef]
5. Sun, K.; Qu, Y.; Wu, Q.; Han, T.T.; Gu, J.W.; Zhao, J.J.; Sun, Y.L.; Jiang, Q.; Gao, Z.Q.; Hu, M.; *et al*. Chemical characteristics of size-resolved aerosols in winter in Beijing. *J. Environ. Sci.* **2014**, *26*, 1641–1650. [CrossRef] [PubMed]
6. Xue, J.; Griffith, S.M.; Yu, X.; Lau, A.K.H.; Yu, J.Z. Effect of nitrate and sulfate relative abundance in $PM_{2.5}$ on liquid water content explored through half-hourly observations of inorganic soluble aerosols at a polluted receptor site. *Atmos. Environ.* **2014**, *99*, 24–31. [CrossRef]
7. Gong, W.; Zhang, T.; Zhu, Z.; Ma, Y.; Ma, X.; Wang, W. Characteristics of $PM_{1.0}$, $PM_{2.5}$, and PM_{10}, and Their Relation to Black Carbon in Wuhan, Central China. *Atmosphere* **2015**, *6*, 1377–1387. [CrossRef]
8. Ram, K.; Sarin, M.M.; Tripathi, S.N. Temporal trends in atmospheric $PM_{2.5}$, PM_{10}, elemental carbon, organic carbon, water-soluble organic carbon, and optical properties: Impact of biomass burning emissions in the Indo-Gangetic Plain. *Environ. Sci. Technol.* **2012**, *46*, 686–695. [CrossRef] [PubMed]
9. Wang, J.; Hu, Z.M.; Chen, Y.Y.; Chen, Z.L.; Xu, S.Y. Contamination characteristics and possible sources of PM_{10} and $PM_{2.5}$ in different functional areas of Shanghai, China. *Atmos. Environ.* **2013**, *68*, 221–229. [CrossRef]
10. Gugamsetty, B.; Wei, H.; Liu, C.N.; Awasthi, A.; Hsu, S.C.; Tsai, C.J.; Roam, G.D.; Wu, Y.C.; Chen, C.F. Source characterization and apportionment of PM_{10}, $PM_{2.5}$ and $PM_{0.1}$ by using positive matrix factorization. *Aerosol Air Qual. Res.* **2012**, *12*, 476–491. [CrossRef]
11. Deshmukh, D.K.; Deb, M.K.; Tsai, Y.I.; Mkoma, S.L. Water soluble ions in $PM_{2.5}$ and PM_1 aerosols in Durg city, Chhattisgarh, India. *Aerosol Air Qual. Res.* **2011**, *11*, 696–708. [CrossRef]
12. An, J.J.; Wang, H.L.; Shen, L.J.; Zhu, B.; Zou, J.N.; Gao, J.H.; Kang, H.Q. Characteristics of new particle formation events in Nanjing, China: Effect of water-soluble ions. *Atmos. Environ.* **2015**, *108*, 32–40. [CrossRef]
13. Reff, A.; Bhave, P.V.; Simon, H.; Pace, T.G.; Pouliot, G.A.; Mobley, J.D.; Houyoux, M. Emissions inventory of $PM_{2.5}$ trace elements across the United States. *Environ. Sci. Technol.* **2009**, *43*, 5790–5796. [CrossRef] [PubMed]
14. Hueglin, C.; Gehrig, R.; Baltensperger, U.; Gysel, M.; Monn, C.; Vonmont, H. Chemical characterisation of $PM_{2.5}$, PM_{10} and coarse particles at urban, near-city and rural sites in Switzerland. *Atmos. Environ.* **2005**, *39*, 637–651. [CrossRef]
15. Yang, D.Y.; Liu, B.X.; Zhang, D.W.; Chen, Y.Y.; Zhou, J.N.; Liang, Y.P. Correlation, Seasonal and Temporal Variation of Water-soluble Ions of $PM_{2.5}$ in Beijing during 2012–2013. *Environ. Sci.* **2015**, *36*, 768–773. (In Chinese).
16. Fann, N.; Lamson, A.D.; Anenberg, S.C.; Wesson, K.; Risley, D.; Hubbell, B.J. Estimating the national public health burden associated with exposure to ambient $PM_{2.5}$ and ozone. *Risk Anal.* **2012**, *32*, 81–95. [CrossRef] [PubMed]

17. Chen, J.; Qiu, S.S.; Shang, J.; Wilfrid, O.M.F.; Liu, X.G.; Tian, H.Z.; Boman, H. Impact of relative humidity and water soluble constituents of $PM_{2.5}$ on visibility impairment in Beijing, China. *Aerosol Air Qual. Res.* **2014**, *14*, 260–268. [CrossRef]
18. Ding, L.; Zhao, W.; Huang, Y.; Cheng, S.; Liu, C. Research on the Coupling Coordination Relationship between Urbanization and the Air Environment: A Case Study of the Area of Wuhan. *Atmosphere* **2015**, *6*, 1539–1558. [CrossRef]
19. Cheng, H.R.; Gong, W.; Wang, Z.W.; Zhang, F.; Wang, X.M.; Lv, X.P.; Liu, J.; Fu, X.X.; Zhang, G. Ionic composition of submicron particles ($PM_{1.0}$) during the long-lasting haze period in January 2013 in Wuhan, central China. *J. Environ. Sci.* **2014**, *26*, 810–817. [CrossRef]
20. Guo, H.T.; Zhou, J.B.; Wang, L.; Zhou, Y.; Yuan, J.P.; Zhao, R.S. Seasonal Variations and Sources of Carboxylic Acids in $PM_{2.5}$ in Wuhan, China. *Aerosol Air Qual. Res.* **2015**, *15*, 517–528. [CrossRef]
21. Cao, J.J.; Shen, Z.X.; Chow, J.C.; Waston, J.G.; Lee, S.C.; Tie, X.X.; Ho, K.F.; Wang, G.H.; Han, Y.M. Winter and summer $PM_{2.5}$ chemical compositions in fourteen Chinese cities. *J. Air Waste Manag.* **2012**, *62*, 1214–1226. [CrossRef]
22. Zhang, F.; Wang, Z.W.; Cheng, H.R.; Lv, X.P.; Gong, W.; Wang, X.M.; Zhang, G. Seasonal variations and chemical characteristics of $PM_{2.5}$ in Wuhan, central China. *Sci. Total. Environ.* **2015**, *518*, 97–105. [CrossRef] [PubMed]
23. Zhang, F.; Cheng, H.R.; Wang, Z.W.; Lu, X.P. Characteristics of Water-soluble Ions in $PM_{2.5}$ during Haze and Non-haze Periods in autumn in Wuhan. *China Power Sci. Technol.* **2013**, *5*, 31–33. (In Chinese). [CrossRef]
24. Wang, Y.; Zhuang, G.S.; Zhang, X.Y.; Huang, K.; Xu, C.; Tang, A.H.; Chen, J.M.; An, Z.S. The ion chemistry, seasonal cycle, and sources of $PM_{2.5}$ and TSP aerosol in Shanghai. *Atmos. Environ.* **2006**, *40*, 2935–2952. [CrossRef]
25. Gu, J.X.; Bai, Z.P.; Li, W.F.; Wu, L.P.; Liu, A.X.; Dong, H.Y.; Xie, Y.Y. Chemical composition of $PM_{2.5}$ during winter in Tianjin, China. *Particuology* **2011**, *9*, 215–221. [CrossRef]
26. Cheng, Y.; Lee, S.C.; Ho, K.F.; Chow, J.C.; Louie, P.K.K.; Cao, J.J.; Hai, X. Chemically-speciated on-road PM 2.5 motor vehicle emission factors in Hong Kong. *Sci. Total. Environ.* **2010**, *408*, 1621–1627. [CrossRef] [PubMed]
27. Tao, J.; Zhang, L.M.; Ho, K.F.; Zhang, R.J.; Lin, Z.J.; Zhang, Z.S.; Lin, M.; Cao, J.J.; Liu, S.X.; Wang, G.H. Impact of $PM_{2.5}$ chemical compositions on aerosol light scattering in Guangzhou—The largest megacity in South China. *Atmos. Res.* **2014**, *135*, 48–58. [CrossRef]
28. Wuhan City Environmental Monitoring Center. Wuhan City Environmental Quality Report. 2014.
29. Lough, G.C.; Schauer, J.J.; Park, J.S.; Shafer, M.M.; Deminter, J.T.; Weinstein, J.P. Emissions of metals associated with motor vehicle roadways. *Environ. Sci. Technol.* **2005**, *39*, 826–836. [CrossRef] [PubMed]
30. Arimoto, R.; Duce, R.A.; Savoie, D.L.; Prospero, J.M.; Talbot, R.; Cullen, D.; Tomza, U. Relationships among aerosol constituents from Asia and the North Pacific during PEM-West A. *J. Geophys. Res.-Atoms.* **1996**, *101*, 2011–2023. [CrossRef]
31. Zhao, Y.N.; Wang, Y.S.; Wen, T.X.; Liu, Q. Characterization of water-soluble ions in $PM_{2.5}$ at Dinghu Mount. *Environ. Sci.* **2013**, *34*, 1232–1239. (In Chinese).
32. Orsini, D.A.; Ma, Y.L.; Sullivan, A.; Sierau, B.; Baumann, K.; Weber, R.J. Refinements to the Particle-Into-Liquid Sampler (PILS) for ground and airborne measurements of water soluble aerosol composition. *Atmos. Environ.* **2003**, *37*, 1243–1259. [CrossRef]
33. Hu, M.; Wu, Z.J.; Slanina, J.; Lin, P.; Liu, S.; Zeng, M. Acidic gases, ammonia and water-soluble ions in $PM_{2.5}$ at a coastal site in the Pearl River Delta, China. *Atmos. Environ.* **2008**, *42*, 6310–6320. [CrossRef]
34. Pathak, R.K.; Chan, C.K. Inter-particle and gas-particle interactions in sampling artifacts of $PM_{2.5}$ in filter-based samplers. *Atmos. Environ.* **2005**, *39*, 1597–1607.
35. Lv, W.; Wang, Y.; Querol, X.; Zhuang, X.; Alastuey, A.; López, A.; Viana, M. Geochemical and statistical analysis of trace metals in atmospheric particulates in Wuhan, central China. *Environ. Geol.* **2006**, *51*, 121–132. [CrossRef]
36. Chen, J.; Qiu, S.; Shang, J.; Wilfrid, O.M.; Liu, X.; Tian, H.; Boman, J. Impact of relative humidity and water soluble constituents of $PM_{2.5}$ on visibility impairment in Beijing, China. *Aerosol Air Qual. Res.* **2014**, *14*, 260–268. [CrossRef]